THE JOURNAL OF PHYSICAL CHEMISTRY B

Article

pubs.acs.org/JPCB

Solvation Properties of Microhydrated Sulfate Anion Clusters: Insights from *ab Initio* Calculations

Quan Wan,[†] Leonardo Spanu,[†] and Giulia Galli*[,†,‡]

[†]Department of Chemistry, University of California, Davis, Davis, California 95616, United States

[‡]Department of Physics, University of California, Davis, Davis, California 95616, United States

Supporting Information

ABSTRACT: Sulfate−water clusters play an important role in environmental and industrial processes, yet open questions remain on their physical and chemical properties. We investigated the smallest hydrated sulfate anion clusters believed to have a full solvation shell, with 12 or 13 water molecules. We used *ab initio* molecular dynamics and electronic structure calculations based on density functional theory, with semilocal and hybrid functionals. At both levels of theory we found that configurations with the anion at the surface of the cluster are energetically favored compared to fully solvated ones, which are instead metastable. We show that infrared spectra of the anion with different solvation shells have similar vibrational signatures, indicating that a mixture of surface and internally solvated geometries are likely to be present in the experimental samples at low temperature. In addition, the computed electronic density of states of surface and internally solvated clusters are hardly distinguishable at finite temperature, with the highest occupied molecular orbital belonging to the anion in all cases. The equilibrium structure determined for $SO_4^{2-}\cdot(H_2O)_{13}$ differs from that previously reported; we find that the addition of one water molecule to a 12-water cluster modifies its hydration shell and that water−water bonds are preferred over water−anion bonds.

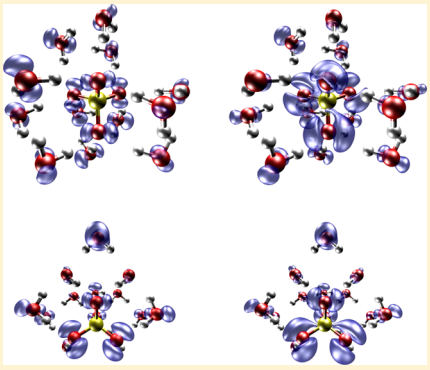

INTRODUCTION

Sulfate−water clusters play an important role in industrial and environmental processes, such as nucleation sites in clouds,[1−4] and the formation of aerosols and thus of acid rain. In addition, sulfate−water clusters are prototype systems for the investigation of the complex structural and dynamical properties of anion solvation.[5,6] For these reasons, small hydrated clusters of the sulfate dianion, $SO_4^{2-}\cdot(H_2O)_n$, have been extensively investigated both experimentally[7−14] and theoretically.[15−20] Isolated sulfate dianion does not exist in the gas phase due to the strong repulsion between its two negative charges, and at least three water molecules are necessary to stabilize the excess charge.[15,21] Blackbody infrared radiative dissociation (BIRD) experiments[12] have shown that $SO_4^{2-}\cdot(H_2O)_6$ and $SO_4^{2-}\cdot(H_2O)_{12}$ clusters are more stable, compared to neighboring ones, and their stability has been interpreted as indicating the presence either of a complete solvation shell or of particularly strong hydrogen bonds. However, a recent theoretical study[20] found several new structures for n = 6−7 that are isoenergetic with the internally solvated anion. Infrared[14] and photodetachment[7,8] experiments on $SO_4^{2-}\cdot(H_2O)_{12}$ have been interpreted as signatures of a complete, symmetric solvation shell around the anion, although neither experiment could lead to unequivocal structural assignments.

Sulfate ions are believed to be absent from air−aqueous solution interfaces.[22] Classical molecular dynamics (MD) simulations of sulfate−water cluster consisting of 60 water molecules suggests a preference for internal solvation of the sulfate dianion.[17] In addition, a joint experimental and theoretical study based on sum frequency generation (SFG) spectroscopy and empirical MD simulations of ammonium and sodium sulfate aqueous solutions[23] and of sulfuric acid[24] in water indicated that at room temperature the sulfate ion is absent within at least 6 Å from the interface with air, in all solutions. However, for small size clusters, such a clear preference for internal solvation is yet unclear.

In this paper we investigate the stability, vibrational and electronic properties of $SO_4^{2-}\cdot(H_2O)_n$ with n = 12 and 13 using *ab initio* molecular dynamics[25,26] and electronic structure calculations[27] based on density functional theory (DFT), with semilocal[28] and hybrid functionals.[29] We considered 12 water molecules, as $SO_4^{2-}\cdot(H_2O)_{12}$ is the most stable among the small sulfate clusters, and it was expected to be the first in the series with a complete solvation shell.[12,14] Both internally and surface solvated structures were investigated. We then added an additional water molecule to investigate in detail the competition between water−water and ion−water interactions. For both 12- and 13-water anion clusters, we studied the stability of different geometrical configurations by computing total energies and vibrational free energies from harmonic frequencies. We then computed infrared (IR) spectra using

Received: April 15, 2012
Revised: July 13, 2012
Published: July 15, 2012

   dx.doi.org/10.1021/jp303624q | *J. Phys. Chem. B* 2012, 116, 9460−9466

both MD simulations and finite difference calculations and compared our results with available infrared multiphoton dissociation (IRMPD) experiments.[14] We found a more complex potential energy surface for the 13-water cluster than previously recognized and obtained similar vibrational signatures for clusters with different structures, making it difficult to use IR spectra to unequivocally assign cluster geometries. Finally, we computed the electronic properties of the internally and surface solvated 12-water sulfate dianion clusters and found very similar electronic density of states and vertical ionization potentials. Our findings are consistent with IR and photodetachment experiments and show that a surface solvated anion configuration is energetically favored, compared to an internally solvated one. We suggest that mixtures of surface and internally solvated configurations may be present in experimental samples, with metastable configurations kinetically trapped in the fast cooling process at low temperature in the case of IRMPD experiments. While structural and stability properties obtained with PBE and PBE0 functionals are similar, the use of a hybrid functional is necessary to obtain quantitative agreement with measured vibrational frequencies and to compute ionization potentials.

The rest of the paper is organized as follows: in the next section we describe our computational methods, and then we present our results, discussing IR spectra of the 12- and 13-water hydrated sulfate anion first, followed by an analysis of their electronic properties. Finally, we present our conclusions in the last section.

THEORETICAL METHODS

We performed *ab initio* Born−Oppenheimer (BO) MD simulations of $SO_4^{2-}\cdot(H_2O)_n$ and $SO_4^{2-}\cdot(D_2O)_n$ clusters with n = 12 and 13, with the generalized-gradient exchange-correlation functional PBE[28] and the hybrid functional PBE0,[29] using the *Qbox* code.[25] We simulated isolated clusters in a cubic super cell of length 30 atomic units (au). The negative charge of the anion was neutralized by a positive uniform background.[30,31] We used plane waves basis sets with a cutoff of 80 Ry and norm-conserving pseudopotentials.[32,33]Our simulations were carried out at 100 K in the NVE ensemble, after equilibrating the system in the constant volume and temperature ensemble (NVT), where the temperature was controlled with a stochastic velocity rescaling thermostat.[34] We used a time step of 5 and 10 au (10 au = 0.24 fs) for light and heavy water, respectively.

Starting from selected configurations from MD trajectories, we optimized the cluster geometries. In the calculation of total energies we included zero-point vibrational energies, obtained using vibrational frequencies determined from harmonic finite difference calculations. We also computed the vertical ionization potential (IP) of selected configurations, defined as $IP = E_{SO_4^{2-}\cdot(H_2O)_n} - E_{SO_4^{-}\cdot(H_2O)_n}$, with both energies computed at the optimized dianion cluster geometry, and using the Makov−Payne correction[35] implemented in the Quantum Espresso code.[27]

Vibrational infrared (IR) spectra were obtained both from finite difference calculations and from dipole dipole correlation functions computed over MD trajectories. The IR intensity (I_k) of a normal mode (Q_k) is proportional to the square of the derivative of the cluster's dipole moment with respect to the normal mode coordinate:[36]

$$I^k \propto \left|\frac{d\vec{\mu}}{dQ_k}\right|^2 = \sum_{i=1}^{N}\sum_{\alpha=1}^{3}\left|\frac{P_{ki,\alpha}}{\sqrt{m_i}}\frac{\partial\vec{\mu}}{\partial r_{i,\alpha}}\right|^2 \quad (1)$$

where $P_{ki,\alpha}$ is the projection of the kth eigenvector of the dynamical matrix onto the αth component of the atomic position $\vec{r}_i$, m_i is the mass of the ith atom, and N is the total number of atoms in the system. The dynamical matrix and the dipole moment derivative $\partial\vec{\mu}/\partial r_i$ can be obtained by finite difference calculations.

IR spectra can also be derived from the Fourier transform of the dipole autocorrelation function computed over an MD trajectory:

$$I(\omega) \propto Q_{QC}\int_{-\infty}^{\infty} dt\ e^{-i\omega t}\langle\vec{\mu}(t)\cdot\vec{\mu}(0)\rangle \quad (2)$$

where the so-called quantum correction term Q_{QC} corrects for the use of the classical expression of the dipole correlation function instead of the quantum mechanical one. Here we adopted the harmonic approximation with $Q_{QC} = \beta\hbar\omega/[1 - \exp(-\beta\hbar\omega)]$,[37−39] which has been extensively used in calculations of IR spectra of bulk water.[40,41] Convergence tests of computed IR spectra as a function of the length of the simulation run are presented in Figure S1 of the Supporting Information. Our results are presented in the next section.

RESULTS AND DISCUSSION

Structural Properties of 12-Water Sulfate Dianion Clusters. We focused on the solvation of the dianion; we did not include solvation studies of HSO_4^- since both IRMPD[14] and photodetachment[7,8] experiments did not detect any signal of OH^-, thus ruling out the occurrence of reactions of SO_4^{2-} with water to form HSO_4^- and OH^-. We considered the two different geometries of $SO_4^{2-}\cdot(H_2O)_{12}$ proposed in refs 12, 16, 14, and 18 and shown in Figure 1. In the 12A structure[12,14,16]

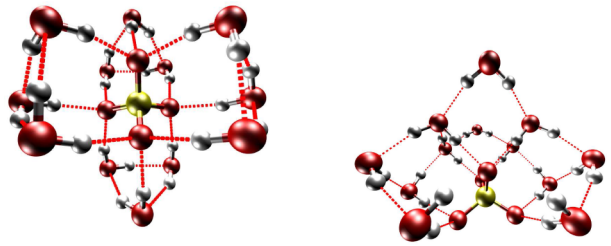

Figure 1. Internally (12A) and surface (12B) solvated configurations of the $SO_4^{2-}\cdot(H_2O)_{12}$ cluster. Oxygen, hydrogen, and sulfur are represented in red, white, and yellow, respectively. Red dotted lines indicate hydrogen bonds.

the sulfate ion is at the center of the cluster; i.e., it is internally solvated, whereas in the 12B configuration[18] all water molecules are on one side of the anion which is thus at the surface of the cluster. The 12A geometry belongs to the T symmetry group. Each water molecule is hydrogen bonded to one oxygen atom of the sulfate ion and to two neighboring water molecules, forming four membered rings, each composed of three molecules. All water molecules reside in a single coordination shell, maximizing the number of hydrogen bonds. On the contrary, the 12B structure has only mirror symmetry, with 8 molecules directly hydrogen-bonded to the anion, forming two

dx.doi.org/10.1021/jp303624q | J. Phys. Chem. B 2012, 116, 9460−9466

four-membered rings (no three-membered rings are present). In these four-membered rings, each molecule has three hydrogen bonds with oxygens of the sulfate anion and one with another water molecule. We note that both three- and four-membered ring structures have been reported in the stable geometries of 6-water sulfate cluster based on IR experiments by Bush et al.;[10] they have also been recently found by Lambrecht et al.[20] in some of the many low-energy geometries of 6- and 7-water sulfate clusters in an exhaustive search for cluster geometries.

In our *ab initio* MD simulations, we found that both 12A and 12B geometries are stable at 100 K (with light and heavy water), for over 20 ps, consistent with the observed stability of 12-water sulfate clusters in BIRD experiments.[12] An analysis of hydrogen bond length and bond angles showed that the 12B structure exhibits shorter hydrogen bonds and larger bond angles than the 12A, indicating the presence of stronger hydrogen bonds than in 12A (see Table 2).

In ref 14 based on the comparison of measured and computed IR spectra, the geometry of the 12A cluster was considered as the most probable one. Photodetachment experiments[7,8] were also interpreted as suggesting the stability of internally solvated configurations for the $SO_4^{2-}\cdot(H_2O)_{12}$ cluster, although these measurements do not permit to make unequivocal structural assignments. However, DFT calculations[18] using the B3LYP exchange and correlation functional found that the 12B geometry is energetically favored over that of 12A by about 0.2 eV.[18] Our total energy calculations with the PBE and PBE0 functionals, inclusive of zero point energies, confirm these findings, as shown in Table 1.

Table 1. Energy Difference (eV) between Cluster Geometries Represented in Figures 1 and 3 for the 12- and 13-Water Hydrated Sulfate Dianion Clusters[a]

geometry	PBE	PBE + ZPE	PBE0	PBE0 + ZPE
12A	0	0	0	0
12B	−0.23	−0.20	−0.19	−0.17
13A	0	0	0	0
13B	−0.28	−0.23	−0.18	−0.14
13C	−0.06	−0.04	−0.05	−0.04

[a]Calculations were carried out using semilocal (PBE) and hybrid (PBE0) functionals and adding the harmonic zero point energy contribution (ZPE) computed from finite difference calculations.

Table 2. Average Bond Lengths (Å) and Average Bond Angles (deg) for Water−Ion and Water−Water Hydrogen Bonds, Computed over 20 ps *ab Initio* MD Trajectories[a]

		12A	12B	13B	13C
bond length	ion−water	1.97	1.84	1.84	1.94
	water−water	1.96	1.94	1.92	1.92
bond angle	ion−water	165.5	168.4	167.7	166.4
	water−water	157.0	163.3	164.8	162.9

[a]No results are shown for 13A, which was found to be unstable in our simulations at finite temperature.

In order to investigate the apparent disagreement between theory and experiments on the cluster stability, we computed IR spectra for the 12A and 12B configurations and compared our results with available IRMPD experiments carried out at 17 K[14] (see Figure 2). We note that IRMPD data are representative of linear IR absorption spectra only under the

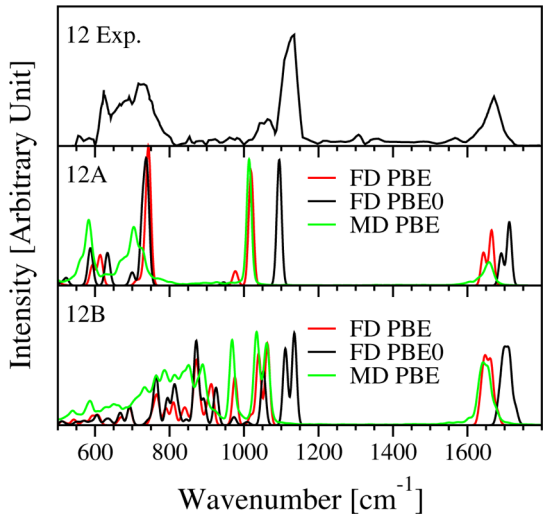

Figure 2. Infrared spectra of 12-water sulfate clusters $SO_4^{2-}\cdot(H_2O)_{12}$. The uppermost panel shows the experimental IRMPD spectra.[14] The middle and lower panels show computed spectra for the 12A and 12B clusters, respectively (see Figure 1), obtained using finite differences (FD) and molecular dynamics (MD) simulations, with either the PBE or PBE0 functional.

assumption of fast internal vibrational redistribution.[5] The accuracy of this hypothesis is difficult to assess, and thus the comparison with experiments presented here is not expected to provide a one-to-one correspondence between computed and measured peaks and it is considered to be qualitative. IR spectra were obtained both from finite difference calculations and from the Fourier transform of the time correlation function of the cluster dipole moment over a ∼20 ps long MD trajectory with light water. In the region between 600 and 800 cm^{-1}, calculated IR spectra for the 12A cluster show a satisfactory agreement with the experimental data. The broad peak within 600−800 cm^{-1} arises from the superposition of the sulfate bending mode at ∼600 cm^{-1} and water librational modes at ∼800 cm^{-1}. In this region of the spectrum we did not find significant differences between results obtained with the PBE and PBE0 functional. IR spectra from MD simulations using PBE show broader features, with librational modes shifted at slightly lower frequencies, compared to those computed from finite differences with the same functional; these differences stem from the inclusion of anharmonic effects in the MD simulations, which appear to be stronger at lower frequency, resulting in a better agreement with experiment. Below 800 cm^{-1}, the agreement between experiments and the computed spectrum of the 12B structure is only fair and inferior to that found for the 12A cluster. However, in the higher frequency region, 1000−1200 cm^{-1}, we found that our results for 12B compare better to experiments than those for 12A. While the 12B structure exhibits peaks both at ∼1100 and 1050 cm^{-1}, similar to experiment, only one sharp peak and a very weak shoulder (close to the main peak) are observed for the 12A cluster. The intense peak at ∼1100 cm^{-1} corresponds to a sulfate stretching mode, which is split in the nonsymmetric 12B cluster; its position is underestimated in PBE calculations by about 80 cm^{-1}, while it is well reproduced using PBE0.

These results suggest that a mixture of symmetric 12A and nonsymmetric 12B sulfate−water clusters are likely to exist in the experimental samples, with the energetically less favorable structure 12A being kinetically trapped under rapid cooling at a

dx.doi.org/10.1021/jp303624q | J. Phys. Chem. B 2012, 116, 9460−9466

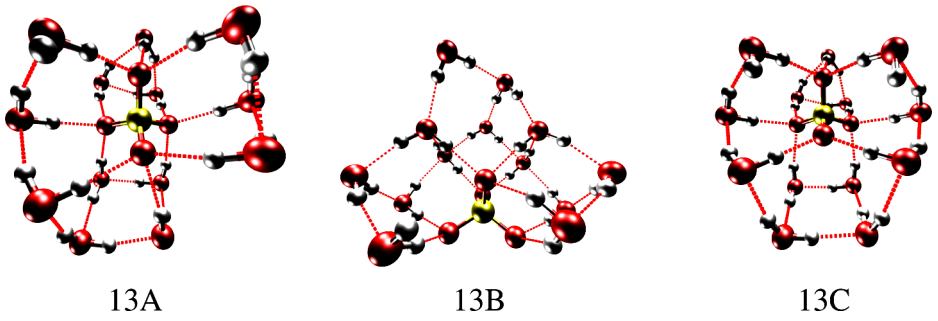

Figure 3. Internally (13A and 13C) and surface (13B) solvated configurations of the $SO_4^{2-}\cdot(H_2O)_{13}$ cluster. Oxygen, hydrogen, and sulfur are represented in red, white, and yellow, respectively. Red dotted lines indicate hydrogen bonds.

very low temperature.[10] This conclusion is also supported by our electronic structure analysis, reported in the electronic structure section. Before discussing the electronic properties, we report below our results for the stability and IR spectra of $SO_4^{2-}\cdot(H_2O)_{13}$.

Structural Properties of 13-Water Sulfate Clusters. We first considered the structure of the 13-water hydrated sulfate cluster denoted as 13A in Figure 3, proposed on the basis of IR experiments;[14] this configuration comprises a water molecule residing in a separate, second solvation shell, while the other 12 molecules remain in the first shell. The calculated IR spectra for the 13A geometry reported in ref 14 show a relatively good agreement with the experimental data, suggesting that 13A may be the stable structure for a 13-water sulfate cluster. The authors of ref 14 therefore concluded that the addition of an extra water molecule to a 12-water sulfate cluster does not affect the structure of the first solvation shell.

We performed MD simulations of a 13-water cluster at 100 K starting from the 13A configuration of Figure 3, and we found that the 13A geometry is not stable. In Figure 4, we report the distance of two water molecules in the first and second coordination shell. After a short simulation time, one of the water molecules leaves the first coordination shell. A similar result was found for both light and heavy water clusters. The new structure found in our MD simulations, denoted as 13C in Figure 3, has a lower energy than the starting one, 13A (see Table 1), after geometry optimization and inclusion of zero point energy. In Figure 5, we report the simulated IR spectra

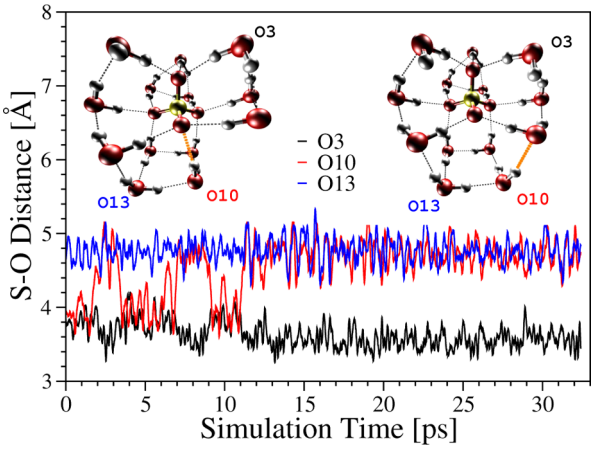

Figure 4. Distance between the sulfur atom and three oxygen atoms (denoted as O3, O10, and O13) belonging to solvating water molecules, during a ~30 ps *ab initio* molecular dynamics simulation at 100 K. The starting (13A) and final (13C) configurations are shown as insets. The bond lengths between S and oxygen atoms 3, 10, and 13 are denoted by black, red, and blue lines, respectively. A jump of O10 from the first to the second solvation shell can be observed from the change in sulfur−oxygen distance: the affected hydrogen bonds are highlighted in orange in both the starting and final configurations.

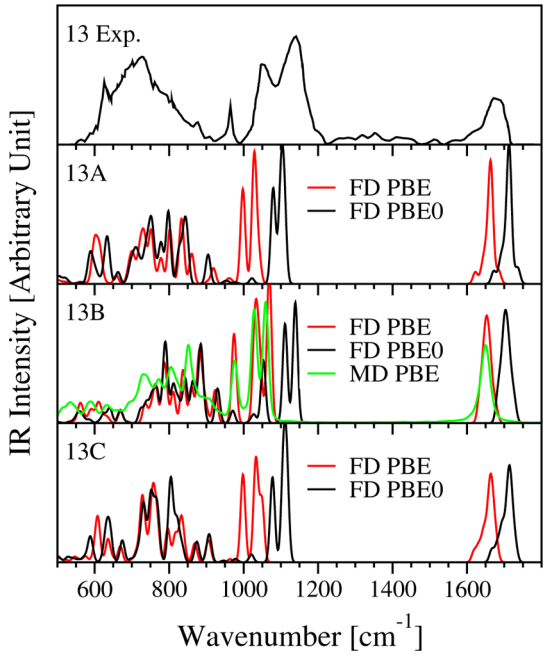

Figure 5. Infrared spectra of 13-water sulfate anion clusters $SO_4^{2-}\cdot(H_2O)_{13}$. The uppermost panel shows the experimental IRMPD spectra.[14] The remaining panels show computed spectra for the 13A, 13B, and 13C clusters, respectively (see Figure 3), obtained using finite differences (FD) and molecular dynamics (MD) simulations, with either the PBE or PBE0 functional.

for 13A and 13C, which turn out to be very similar. Zhou et al.[14] assumed the existence of 13A under experimental conditions based on the peak at 965 cm^{-1}, attributed to a vibrational mode localized on the water molecule outside the first solvation shell. Our results show that rather different geometries of the solvation shells exhibit almost identical IR spectra, in particular the same peak at 965 cm^{-1}. These findings indicate that the geometry of the solvated dianion cannot be unequivocally determined based solely on IR experiments.

To further investigate the stability of the first solvation shell, we simulated a 13-light-water cluster starting from the 12B geometry with one extra water molecule (see Figure 6). We started our simulation by placing the extra water molecule close

dx.doi.org/10.1021/jp303624q | J. Phys. Chem. B 2012, 116, 9460−9466

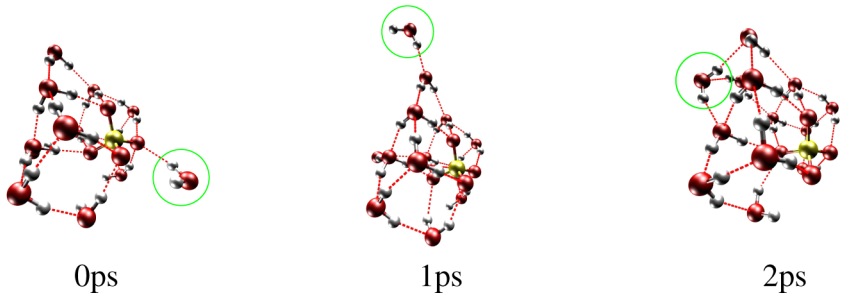

Figure 6. Structural changes observed during the first 2 ps of an *ab initio* MD simulation of a 13-water hydrated sulfate anion cluster (see text).

to the bare side of the anion. After a short simulation time (~2 ps), the extra water molecule (circled in green in Figure 6) migrates to the opposite side of the cluster, leaving the anion at the surface. The new surface-solvated configuration is labeled 13B in Figure 3. The extra water molecule does not bind to the anion, but rather it prefers to form hydrogen bonds with the other water molecules (see also Table 2). This preference for water molecules to bind with water rather than the sulfate anion was also predicted by calculations[18,20] of smaller sulfate clusters. The configuration 13B is energetically favored with respect to 13A and 13C (see Table 1) by about 0.15 eV, an energy difference of the same order as that found between 12A and 12B.

Simulated IR spectra for 13B are shown in Figure 5. Similarities are evident in the IR features of 12B and 13B, especially in the splitting of the sulfate streching mode in the 1000−1100 cm^{-1} region. All the three structures investigated here, 13A, 13B, and 13C, show IR spectra with features that match experimental measurements. Overall our findings indicate that for $SO_4^{2-}\cdot(H_2O)_n$ clusters with n = 12 and 13, configurations where the anion is at the surface are expected to be present in experimental samples, likely in a mixture of internally and surface solvated geometries. We now turn to the discussion of the cluster electronic properties and show that our results on surface solvation are also consistent with photodetachment data, although photodetachment experiments have been interpreted as showing internal solvation of the anion in $SO_4^{2-}\cdot(H_2O)_{12}$.

Electronic Properties. The description of the electronic properties of solvated anions is in general more complex than that of simple cations. For example, it has been shown[42,43] that local and semilocal exchange and correlation functionals incorrectly describe the charge distribution around negative ions in water, e.g. Cl^-, yielding a delocalized charge distributed over the first shell of solvating water molecules. The use of hybrid functionals that include a portion of Hartree−Fock exact exchange may alleviate this problem and lead to a better localization of the charge around the anion.

We computed

$$\Delta\rho = \rho_{SO_4^{2-}\cdot(H_2O)_n} - \rho_{SO_4^{-}\cdot(H_2O)_n} \quad (3)$$

where $\rho_{SO_4^{2-}\cdot(H_2O)_n}$ is the charge density of the original cluster and $\rho_{SO_4^{-}\cdot(H_2O)_n}$ the charge density of a cluster with one eletron removed. Our results are reported in Figure 7. $\Delta\rho$ may be regarded as the probability distribution of the quasi-particle HOMO of the system and describes the most probable distribution of the electron that is removed from the doubly charged cluster in a vertical ionization process. This charge distribution is in general different from that of the Kohn−Sham orbital corresponding to the highest eigenvalue in a DFT calculation.

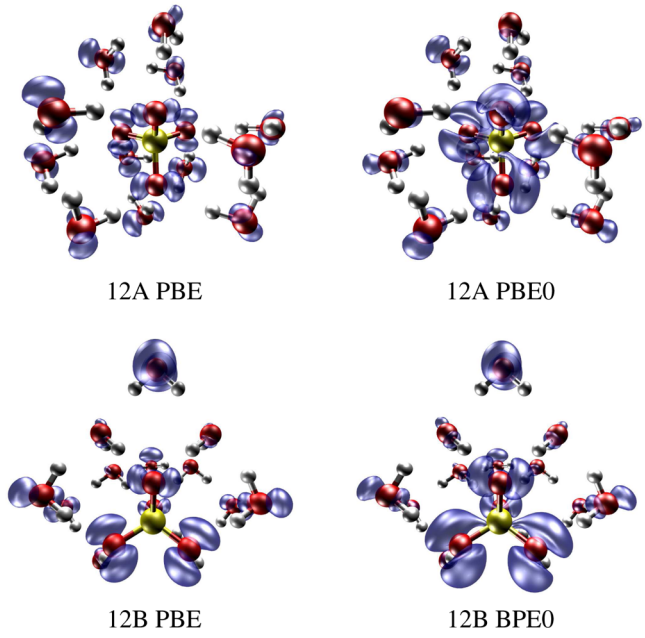

Figure 7. Charge density differences between the 12-water hydrated SO_4^{2-} and SO_4^{-} clusters in the 12A (two upper panels) and 12B (two lower panels) configurations (see Figure 1), obtained using the PBE (left panels) and PBE0 (right panels) functionals. Note the difference in charge localization obtained with semilocal and hybrid functionals. The same value of charge density is plotted in all cases.

Similar to results reported for Cl^-,[42] when using PBE $\Delta\rho$ is partially delocalized over the water molecules around the anion, for both the 12A and 12B configurations (see left panel of Figure 7). The use of PBE0 leads instead to a more localized charge distribution around the sulfate (see right panel of Figure 7).

One expects a higher bond order for the S−O bond and a higher vibrational frequency for its stretching mode when the electronic charge is more localized on the anion. Indeed, our calculated IR spectra (Figures 2 and 5) obtained with the PBE0 functional show a sulfate stretching mode at a higher frequency than PBE calculations and in much better agreement with experiments. We note that the position of the sulfate stretching mode at 1100 cm^{-1} is a good indicator of the accuracy of the theory, as this peak appears to be decoupled from other water and sulfate vibrational modes. In addition, nuclear quantum effects may be regarded as negligible in this case, as only S and O atoms contribute to the mode.

dx.doi.org/10.1021/jp303624q | J. Phys. Chem. B 2012, 116, 9460−9466

In Table 3, we report the calculated vertical ionization potential (IP) of the 12 water cluster, defined as IP = $E_{SO_4^{2-}\cdot(H_2O)_n} - E_{SO_4^{-}\cdot(H_2O)_n}$. As expected, the IP obtained within PBE0 is higher than the value obtained at the PBE level of theory and in better agreement with the experimental value of ~3.7 eV estimated from the position of the outermost peak of the photodetachment spectrum.[8]

Table 3. Calculated Vertical Ionization Potential (eV) of 12A and 12B Sulfate Dianion Clusters (See Figure 1), Obtained with Semilocal (PBE) and Hybrid (PBE0) Functionals

functional	12A	12B
PBE	2.9	2.6
PBE0	3.9	3.6

The computed value for 12B appears to be in better agreement with experiments, suggesting that this configuration may be the most probable one found in photodetachment experiments. However, it is unclear whether the accuracy of the theory at the PBE0 level is sufficient for a definite assignment of the geometry based on computed IP compared to experiments. In addition, the computed vertical IPs of 12A and 12B differ by only 0.3 eV and the experimental peaks are rather broad (roughly 1 eV), since the experiments were performed at room temperature. Most likely the experimental samples contain an ensemble of various configurations.

We also computed the electronic density of states (EDOS) of the 12A and 12B geometries: these are shown in Figure 8, where we drew green and black arrows in correspondence of peaks predominantly arising from anion states and from water states, respectively. PBE and PBE0 calculations yield similar EDOS distributions; however, the energy separation between the uppermost anion and water states is substantially larger at the PBE0 level, indicating, as expected, a different level alignment between anion and water states at the two levels of theory. Interestingly, the EDOS of the 12A and 12B geometries are also rather similar: in both cases the uppermost peak belongs to the anion, followed by water states, and then by an anion state about 1.8 eV lower in energy than the outermost one. Although a direct comparison between EDOS and photodetachment spectra is not possible (as no information about escape barriers is contained in the computed EDOS), our results strongly suggest that it is not possible to discern between internally solvated and surface solvated geometries of the 12-water hydrated dianion on the basis of photodetachment experiments at room temperature.

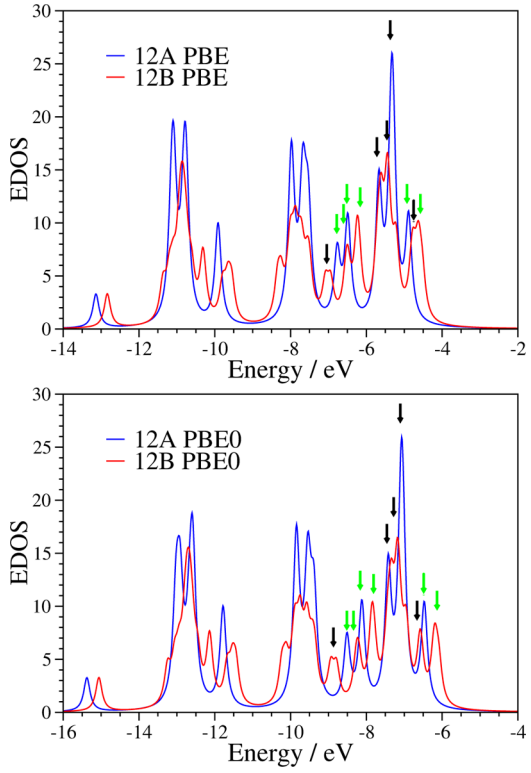

Figure 8. Electronic density of states (EDOS) of the 12A and 12B (Figure 1) computed using the PBE (upper panel) and PBE0 (lower panel) exchange-correlation functionals. Green and black arrows indicate the first three orbitals belonging to sulfate ion, water, and sulfate ion, respectively (see text).

Finally, we computed the vertical ionization potential using the PBE0 functional and the PBE single particle orbitals and vice versa. The results showed insensitivity to the orbitals used and a strong dependence on the functional, consistent with the findings of ref 43. Therefore, $\Delta\rho$ appears to be a reliable indicator of the accuracy of the theory for electronic properties calculations. We note that despite inaccurate results for ionization potentials and the fair predictions of vibrational frequencies, PBE can still provide qualitatively correct results on the structural properties and the overall shape of IR spectra.

CONCLUSIONS

We revisited the interpretation of spectroscopic (IR) and photodetachment experiments on hydrated sulfate anions with 12 and 13 water molecules. $SO_4^{2-}\cdot(H_2O)_{12}$ is a particularly stable cluster and was believed to be the first one of the series to present a full hydration shell. We also considered an additional water molecule (that is, $SO_4^{2-}\cdot(H_2O)_{13}$) to investigate in detail the competing water−water and water−anion interactions. Using *ab initio* MD and electronic structure calculations, we found that at zero temperature, surface hydrated configurations are more stable than fully solvated ones for both the 12- and 13-water clusters, by about 0.15 eV. Computed IR spectra suggest that at low temperature the samples produced in IRMPD experiments are likely to contain an ensemble of surface and internally solvated geometries, with the less stable ones being kinetically trapped. Computed electronic density of states and ionization potentials for surface solvated and internally hydrated clusters are both fully consistent with photodetachment experiments conducted at room temperature. Therefore, these experiments may not be used to discern between the different cluster geometries for the small cluster sizes considered here. Likewise, IR spectra may not be used to make definitive structural assignments as we found that different geometries may have similar vibrational signatures, with striking similarities especially in the case of 13-water clusters. It was previously reported that adding a water molecule to $SO_4^{2-}\cdot(H_2O)_{12}$ has a negligible influence on its first solvation shell. However, our MD simulations showed that the presence of an extra molecule does affect the cluster. Our calculations indicate that it is only in clusters larger than previously believed that one observes a clear preference for internal solvation of the sulfate dianion and that surface solvated geometries are likely to be present, possibly as the majority population, in several experiments with small clusters.

dx.doi.org/10.1021/jp303624q | J. Phys. Chem. B 2012, 116, 9460−9466

Since internally and surface solvated clusters behave differently as nucleation sites in water droplets, our results may have implications in understanding aerosol processes that involve sulfate dianion. Finally, we note that PBE0 calculations are superior to PBE ones in describing vibrational spectra and ionization potentials. However, we found that PBE does provide qualitatively correct results on the structural properties and overall shape of IR spectra.

■ ASSOCIATED CONTENT

Supporting Information

Figure S1. This material is available free of charge via the Internet at http://pubs.acs.org.

■ AUTHOR INFORMATION

Corresponding Author

*E-mail: gagalli@ucdavis.edu.

Notes

The authors declare no competing financial interest.

■ ACKNOWLEDGMENTS

We thank F. Gygi and C. Zhang for useful discussions. This work was supported by NSF Grant OCI-074921 and Shell Corporation. ALCF computational resources at Argonne National Laboratory and UC ShaRCS computational resources are gratefully acknowledged.

■ REFERENCES

(1) Abbatt, J. P. D.; Benz, S.; Cziczo, D. J.; Kanji, Z.; Lohmann, U.; Möhler, O. *Science* **2006**, *313*, 1770−3.
(2) Ramanathan, V.; Crutzen, P.; Kiehl, J.; Rosenfeld, D. *Science* **2001**, *294*, 2119.
(3) Harrison, R. G.; Carslaw, K. S. *Rev. Geophys.* **2003**, *41*, 1012.
(4) Yu, F.; Turco, R. P. *J. Geophys. Res.* **2001**, *106*, 4797−4814.
(5) Asmis, K. R.; Neumark, D. M. *Acc. Chem. Res.* **2012**, *45*, 43−52.
(6) Tielrooij, K.; Garcia-Araez, N.; Bonn, M.; Bakker, H. *Science* **2010**, *328*, 1006.
(7) Wang, X.; Yang, X.; Nicholas, J.; Wang, L. *Science* **2001**, *294*, 1322.
(8) Yang, X.; Wang, X.; Wang, L. *J. Phys. Chem. A* **2002**, *106*, 7607−7616.
(9) Wang, X.-B.; Sergeeva, A. P.; Yang, J.; Xing, X.-P.; Boldyrev, A. I.; Wang, L.-S. *J. Phys. Chem. A* **2009**, *113*, 5567−5576.
(10) Bush, M.; Saykally, R.; Williams, E. *J. Am. Chem. Soc.* **2007**, *129*, 2220−2221.
(11) O'Brien, J. T.; Prell, J. S.; Bush, M. F.; Williams, E. R. *J. Am. Chem. Soc.* **2010**, *132*, 8248−8249.
(12) Wong, R. L.; Williams, E. R. *J. Phys. Chem. A* **2003**, *107*, 10976−10983.
(13) Blades, A. T.; Kebarle, P. *J. Phys. Chem. A* **2005**, *109*, 8293−8.
(14) Zhou, J.; Santambrogio, G.; Brümmer, M.; Moore, D. T.; Wöste, L.; Meijer, G.; Neumark, D. M.; Asmis, K. R. *J. Chem. Phys.* **2006**, *125*, 111102.
(15) Wang, X.-B.; Nicholas, J. B. *Chem. Phys.* **2000**, *113*, 10837−10840.
(16) Zhan, C.-G.; Zheng, F.; Dixon, D. A. *J. Chem. Phys.* **2003**, *119*, 781.
(17) Jungwirth, P.; Curtis, J. *Chem. Phys. Lett.* **2003**, *367*, 704−710.
(18) Gao, B.; Liu, Z.-F. *J. Chem. Phys.* **2004**, *121*, 8299−8306.
(19) Gao, B.; Liu, Z.-F. *J. Chem. Phys.* **2005**, *123*, 224302.
(20) Lambrecht, D.; Clark, G.; Head-Gordon, T.; Head-Gordon, M. *J. Phys. Chem. A* **2011**, *4*, 11438−11454.
(21) Boldyrev, A.; Simons, J. *J. Phys. Chem.* **1994**, *98*, 2298−2300.
(22) Jungwirth, P.; Tobias, D. J. *Chem. Rev.* **2006**, *106*, 1259−1281.
(23) Gopalakrishnan, S.; Jungwirth, P.; Tobias, D. J.; Allen, H. C. *J. Phys. Chem. B* **2005**, *109*, 8861−8872.
(24) Ishiyama, T.; Morita, A. *J. Phys. Chem. C* **2011**, *115*, 13704−13716.
(25) Qbox Code: http://eslab.ucdavis.edu/software/qbox/.
(26) Car, R.; Parrinello, M. *Phys. Rev. Lett.* **1985**, *55*, 2471−2474.
(27) Giannozzi, P.; Baroni, S.; Bonini, N.; Calandra, M.; Car, R.; Cavazzoni, C.; Ceresoli, D.; Chiarotti, G.; Cococcioni, M.; Dabo, I.; et al. *J. Phys.: Condens. Matter* **2009**, *21*, 395502.
(28) Perdew, J.; Burke, K.; Ernzerhof, M. *Phys. Rev. Lett.* **1996**, *77*, 3865−3868.
(29) Adamo, C.; Barone, V. *J. Chem. Phys.* **1999**, *110*, 6158.
(30) In periodic boundary condition calculations of a charged system, a background charge is used to neutralize the net charge in the unit cell so as to avoid divergence of electrostatic terms in the Hamiltonian.
(31) Martin, R. *Electronic Structure: Basic Theory and Practical Methods*; Cambridge University Press: New York, 2004.
(32) Pseudopotential table: http://fpmd.ucdavis.edu/potentials.
(33) Vanderbilt, D. *Phys. Rev. B* **1985**, *32*, 8412−8415.
(34) Bussi, G.; Donadio, D.; Parrinello, M. *J. Chem. Phys.* **2007**, *126*, 014101.
(35) Makov, G.; Payne, M. *Phys. Rev. B* **1995**, *51*, 4014.
(36) Carrasco, J.; Michaelides, A.; Forster, M.; Haq, S.; Raval, R.; Hodgson, A. *Nat. Mater.* **2009**, *8*, 427−31.
(37) Egorov, S. A.; Everitt, K. F.; Skinner, J. L. *J. Phys. Chem. A* **1999**, *103*, 9494−9499.
(38) Egorov, S. A.; Skinner, J. L. *Chem. Phys. Lett.* **1998**, *293*, 469−476.
(39) Ramírez, R.; López-Ciudad, T.; Kumar, P, P.; Marx, D. *J. Chem. Phys.* **2004**, *121*, 3973−83.
(40) Sharma, M.; Resta, R.; Car, R. *Phys. Rev. Lett.* **2005**, *95*, 187401.
(41) Zhang, C.; Donadio, D.; Galli, G. *J. Phys. Chem. Lett.* **2010**, *1*, 1398−1402.
(42) Cohen, A.; Mori-Sánchez, P.; Yang, W. *Science* **2008**, *321*, 792.
(43) Cohen, A. J.; Mori-Sánchez, P.; Yang, W. *Chem. Rev.* **2012**, *112*, 289−320.